ISSN 0022-4766, Journal of Structural Chemistry, 2020, Vol. 61, No. 7, pp. 1124-1131. © Pleiades Publishing, Ltd., 2020.
Text © The Author(s), 2020, published in Zhurnal Strukturnoi Khimii, 2020, Vol. 61, No. 7, pp. 1186-1194.

STRUCTURAL INSIGHTS AND ANTI-COLON CANCER ACTIVITY OF TWO Zn(II)-BASED COORDINATION POLYMERS BASED ON CARBOXYLATE AND IMIDAZOLE CO-LIGANDS

Y. Yang[1], P. Li[2]*, and S.-H. Li[3]

Two new mixed-ligand coordination polymers $[Zn(bdc)(bib)]_n$ (**1**, H_2bdc = 1,3-dicarboxybenzene, bib = 1,3-bis(imidazol-1-yl)benzene) and $[Zn(NH_2\text{-}bdc)(bib)]_n$ (**2**, NH_2–H_2bdc = 2-amino-1,4-dicarboxylbenzene) are successfully prepared by the reaction of zinc nitrate, N-containing and dicarboxylate ligands under the same hydrothermal conditions. The anti-viability of compounds **1** and **2** is assessed with CCK-8 against SW480 colon cancer cells. To further explore the underlying mechanism of compounds, the cell apoptosis and ROS detection are performed in this experiment.

DOI: 10.1134/S0022476620070161

Keywords: coordination polymer, mixed-ligand, X-ray, colon cancer cell.

INTRODUCTION

Cancer is the second leading cause of human death after cardiovascular and cerebrovascular diseases, especially in the developing and the undeveloped countries. According to the article published in the CA magazine "Global Cancer Statistics, 2012", there were 14 million new cancer cases in the world in 2012 [1]. Metal complexes constitute an important class of compounds of biological interest because of their natural propensity to interact with DNA [2]. Due to their cationic characteristics, a wide spectrum of ligands, a broad range of structural geometries and electronic properties as well as kinetic properties and mechanisms of drug action, metal complexes have been widely studied and potentially used in gene regulation, probing of DNA specific structures and interactions, and the design of therapeutic agents [3-5].

As a unique class of crystalline materials constructed via self-assembly of metal ions/clusters and organic ligands, coordination polymers (CPs) have rapidly emerged in chemistry and materials science due to their new topological structures as well as versatile potential applications such as gas storage/separation, catalysis, magnetism, optics, and chemical sensing [6-10]. However, the rational design and synthesis of CPs with targeted properties and functionality have been a challenge for the synthetic chemistry. In general, the self-assembly of well-designed metal ions/clusters nodes and organic ligands is one of the most effective and available methods for preparing targeted CPs. Among various organic ligands, aromatic dicarboxylates and bis(imidazolyl)-substituted ligands are common linkers for constructing CPs [11-13]. The construction of CPs with the

[1]Department of Gastrointestinal and Abdominal Hernia Surgery, People's Hospital of Jinxiang County, Jinxiang, Shandong, P. R. China. [2]Department of General Surgery, The Seventh People's Hospital of Chongqing, Chongqing, P. R. China; *peilin_li11@126.com. [3]Department of Medicine, Affiliated Hospital of Sun Yat-sen University, Guangzhou, Guangdong, P. R. China. Original article submitted October 8, 2019; revised November 26, 2019; accepted January 16, 2020.

flexible ligands is propitious to produce versatile structures and/or structural transformations by external stimuli, while the rigid ones enable the preparation of stable CPs, offering permanent porosity. In addition, the shape of organic ligands also affects the topology of targeted CPs. On the other hand, the self-assembly of CPs is influenced by many factors, such as metal-to-ligand molar ratios, coordination abilities of the ligands, the types of metal ions and solvent molecules, reaction temperatures, counter ions, pH values of the reaction systems and reaction medium, etc. Therefore, the investigation of the relationship between reaction conditions and the final structures can lead us to the design and synthesis of CPs with fantastic structures [14-18]. In this study, two new mixed-ligand CPs $[Zn(bdc)(bib)]_n$ (**1**, H_2bdc = 1,3-dicarboxybenzene, bib = 1,3-bis(imidazol-1-yl)benzene) and $[Zn(NH_2\text{-}bdc)(bib)]_n$ (**2**, NH_2–H_2bdc = 2-amino-1,4-dicarboxybenzene) have been successfully prepared by the reaction of zinc nitrate, N-containing and dicarboxylate ligands under the same hydrothermal conditions. The CCK-8 results suggested that compound **1** exhibited the outstanding anticancer activity rather than compound **2**. Moreover, the apoptosis detection indicated that compound **1** significantly induced the apoptosis production in SW480 colon cancer cells, and the ROS measurement proved the apoptosis to be initiated by the up-regulation of ROS in cancer cells.

EXPERIMENTAL

Chemicals and measurements. The chemicals as well as reagents were purchased from Beijing Bailingwei Reagent Company and Tianjin Guangfu Chemical Reagent Company, and they were used without further purification. We utilized the Elementar Vario Micro elemental analyzer for the N, C, H content.

Preparation and characterization of $[Zn(bdc)(bib)]_n$ (1) and $[Zn(NH_2\text{-}bdc)(bib)]_n$ (2). For complex **1**, a mixture of bib (21.2 mg, 0.1 mmol), H_2bdc (17 mg, 0.1 mmol), and $Zn(NO_3)_2{\cdot}6H_2O$ (29.7 mg, 0.1 mmol) was dissolved in 5 mL of a DMF–MeOH–H_2O (3/1/1) solvent in a glass vial (10 mL) and stirred for 30 min. The vessel was placed in an oven and heated at 85 °C for 5 days. And then the reaction mixture was cooled to room temperature. Colorless block crystals of **1** were isolated by filtration, washed with EtOH, and dried in air. The yield was about 62% (14.01 mg) based on the bib ligand. Anal. calcd for $C_{20}H_{14}N_4O_4Zn$ (%): C 54.63, H 3.21, N 12.74. Found (%): C 54.56, H 3.78, N 12.92.

For complex **2**, a mixture of bib (21.2 mg, 0.1 mmol), NH_2–H_2bdc (19 mg, 0.1 mmol), and $Zn(NO_3)_2{\cdot}6H_2O$ (29.7 mg, 0.1 mmol) was dissolved in 5 mL of a DMF–MeOH–H_2O (3/1/1) solvent in a glass vial (10 mL) and stirred for 30 min. The vessel was placed in an oven and heated at 85 °C for 5 days. And then the reaction mixture was cooled to room temperature. Yellow block crystals were isolated by filtration, washed with EtOH, and dried in air. The yield was about 48% (11.9 mg) based on the bib ligand. Anal. calcd for $C_{20}H_{15}N_5O_4Zn$ (%): C 52.82, H 3.32, N 15.40. Found (%): C 52.56, H 3.78, N 15.62.

The X-ray data were obtained on the Oxford Xcalibur E diffractometer with MoK_α radiation (λ = 0.71073 Å). The intensity data were analyzed using the CrysAlisPro software and converted to the HKL files. The olex2.solve embedded in the OLEX 2 software was used to get the structural models, and the SHELXL-2014 program based on the least-squares approach was modified [19-21]. All non-H atoms were mixed with anisotropic parameters. Then we utilized the AFIX commands to fix all H atoms geometrically on the C atoms to which they are attached. Table 1 summarizes the refinement details as well as crystallographic parameters of the two complexes.

Cell viability analysis. Stock solutions of compounds **1** and **2** were prepared in DMSO (Sigma Aldrich) at a concentration of 1000 μg/mL via grinding the crystalline samples in a mortar with a pestle for 1 h and then treated via ultrasound. The powders were sterilized by filtration through Millipore filter (0.22 μM) before use, and diluted by the cell culture medium to various working concentrations. The cell viability of SW480 colon cancer cells treated with the compounds was determined with the CCK-8 detection kit as described previously. In short, the SW480 cells were seeded onto 96-well plates with a density of $1{\cdot}10^3$ cells/well in a volume of 100 μL. When the cells stepped into the logarithmic growth phase and reached a 70-80% confluence, compounds **1** and **2** (1 μg/mL, 2 μg/mL, 4 μg/mL, 8 μg/mL, 10 μg/mL, 20 μg/mL, 40 μg/mL, 80 μg/mL) were added for 24 h incubation. At the end of incubation, the cell medium was discarded

TABLE 1. Refinement Details and Crystallographic Parameters for Complexes **1** and **2**

Parameter	**1**	**2**
Empirical formula	$C_{20}H_{14}N_4O_4Zn$	$C_{20}H_{15}N_5O_4Zn$
Formula weight	439.74	454.74
Temperature, K	296.15	273
Crystal system	Monoclinic	Tetragonal
Space group	$P2_1/c$	$P4_3$
a, b, c, Å	12.363(4), 13.164(6), 13.986(6)	8.9631(2), 8.9631(2), 22.0692(7)
β, deg	111.023(2)	90
V, Å^3	2124.6(15)	1772.98(11)
Z	4	4
ρ_{calc}, g/cm^3	1.375	1.704
μ, mm^{-1}	1.187	1.428
Data / restraints / parameters	4178 / 0 / 262	3417 / 1 / 271
GOOF on F^2	1.119	1.003
Final R indexes (I ≥ 2σ(I)]	R_1 = 0.0460, wR_2 = 0.1479	R_1 = 0.0412, wR_2 = 0.1098
Final R indexes (all data)	R_1 = 0.0489, wR_2 = 0.1495	R_1 = 0.0648, wR_2 = 0.1177
Largest diff. peak / hole, e/Å^3	0.73 / –0.69	0.44 / –0.49
CCDC	1967177	1967178

and replaced with a CCK-8 solution in 100 μL of the culture medium. Finally, the optical density (OD) values were measured at 490 nm using a microplate reader (Bio-Rad, Hercules, CA). Cell viability (%) was calculated according to the following formula: viability (%) = $(OD_{sample} - OD_{blank})/(OD_{control} - OD_{blank})\cdot 100$.

Cell apoptosis analyzed by flow cytometry. The Annexin V-FITC Apoptosis Detection kit was applied for the SW480 cell apoptosis determination according to the protocol described previously. In brief, the SW480 of $2\cdot10^5$ cells/well were seeded into six-well plates and cultured at a 37 °C, 5% CO_2 incubator overnight. Then, serious dilutions of compounds **1** and **2** were added to cells for 24 h treatment. Subsequently, the SW480 cells were trypsinized, harvested, washed three times with PBS and stained with 5 μL of Annexin V-FITC and 5 μL of propidium iodide (PI) for 10 min in dark at room temperature. Finally, the cell samples were analyzed by flow cytometry immediately (FACSVerse, BD, San Jose, CA) and the CellQuest software (FACSCalibur). All experiments were repeated three times.

Intracellular ROS detection. The intracellular ROS accumulation of SW480 cells after treatment with compounds **1** and **2** was measured by the DCFH-DA assay following the protocols. Briefly, the SW480 cells were planted onto six-well plates at the density of $2\cdot10^5$ cells per well and cultivated at a 37 °C, 5% CO_2 wet environment. After that, different concentrations of compounds **1** and **2** were used for cancer cell treatment. After 24 h treatment, the SW480 cells were harvested and incubated with 10 μM DCFH-DA solution for 30 min at 7 °C, 5% CO_2. The ROS level was determined by a flow cytometer.

RESULTS AND DISCUSSION

Molecular structures. Complex **1** could be prepared by the solvothermal reaction of bib, H_2bdc, and $Zn(NO_3)_2\cdot6H_2O$ (29.7 mg, 0.1 mmol) in a mixed DMF–MeOH–H_2O solvent at 85 °C for 5 days. The single crystal X-ray diffraction analysis indicates that complex **1** crystallizes in the monoclinic space group $P2_1/c$ with an asymmetric unit consisting of a divalent Zn(II) atom, a 1,3-bib ligand, and a fully deprotonated H_2bdc ligand. As shown in Fig. 1*a*, the coordination sphere of the Zn atom consists of two O donor atoms from two different bdc^{2-} ligands, with

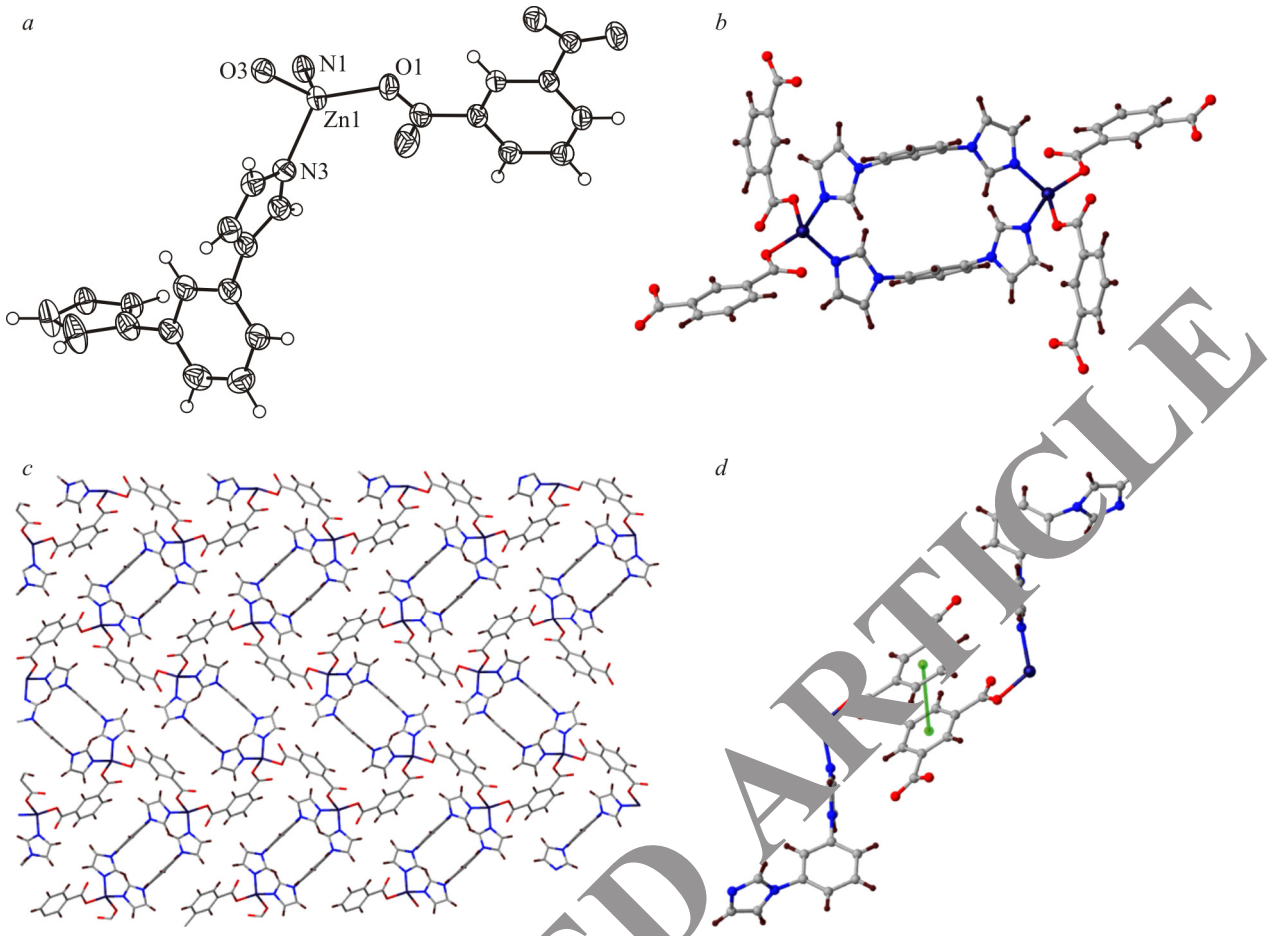

Fig. 1. Basic repeating unit for **1** (*a*); $[Zn_2(1,3\text{-bib})_2]_n$ clusters connected via the bdc^{2-} ligand (*b*); 2D layered network of **1** (*c*); π–π stacking interaction between the adjacent bdc^{2-} ligands in the adjacent layers (*d*).

Zn1–O1 = 1.951(14) Å and Zn1–$O3^{i}$ = 1.954(14) Å (symmetry code: ^{i} *x*+1, *y*–1/2, –*z*+1/2) and two N atoms from two different 1,3-bib ligands, with Zn1–N1 = 2.0326(16) Å and Zn1–$N4^{iv}$ = 2.032(18) Å (symmetry code: ^{iv} –*x*+2, –*y*, –*z*+1). A distorted tetrahedral $\{ZnN_2O_2\}$ coordination environment is evident with $\tau_4 = 0.87$ ($\tau_4 = 360 - (\alpha + \beta)/141°$ where α and β are the two largest bond angles in the four-coordination compound). Neighboring Zn(II) atoms are bridged by 1,3-bib ligands to form $[Zn_2(1,3\text{-bib})_2]_n$ clusters with a Zn···Zn distance of 10.434(9) Å (Fig. 1*b*). Zn(II) ions are bridged by bdc^{2-} ligands to generate a 1D left-handed $[Zn(bdc)]_n$ single helical chain with a pitch of 13.324(1) Å; the distance between two adjacent Zn(II) ions is 8.126(2) Å and the Zn–Zn–Zn angle is 110.015(6)°. In addition, another one-dimensional (1D) right-handed $[Zn(bdc)]_n$ single helical chain is also formed in the structure of **1**. Furthermore, these 1D left- and right-handed helical chains are connected by $[Zn_2(1,3\text{-bib})_2]_n$ clusters to generate a 2D framework oriented parallel to the (102) crystal planes (Fig. 1*c*). Further insight into the nature of this intricate framework can be acquired using the topological analysis, which was performed with the TOPOS software. From a topological point of view, if the $[Zn_2(bib)_2]_n$ clusters are considered as 4-connected nodes, the bdc^{2-} ligands are reduced to linkers and the whole framework can be simplified as a 4-connected network with a (4,4) topology. The structure of **1** is further stabilized by the π–π stacking interaction between the adjacent bdc^{2-} ligands in the adjacent layers with a distance of 3.791(2) Å (Fig. 1*d*).

Complex **2** crystallizes in the tetragonal space group $P4_3$. As shown in Fig. 2*a*, the asymmetric unit consists of one crystallographically independent Zn(II) ion, one partially deprotonated NH_2-bdc^{2-} ligand, and one neutral bib ligand, all of which contribute to a neutral framework structure. The coordination environment of the central metal Zn(II) ion and the coordination modes of ligands are similar to that of complex **1**, which is completed by two carboxylate O atoms from two

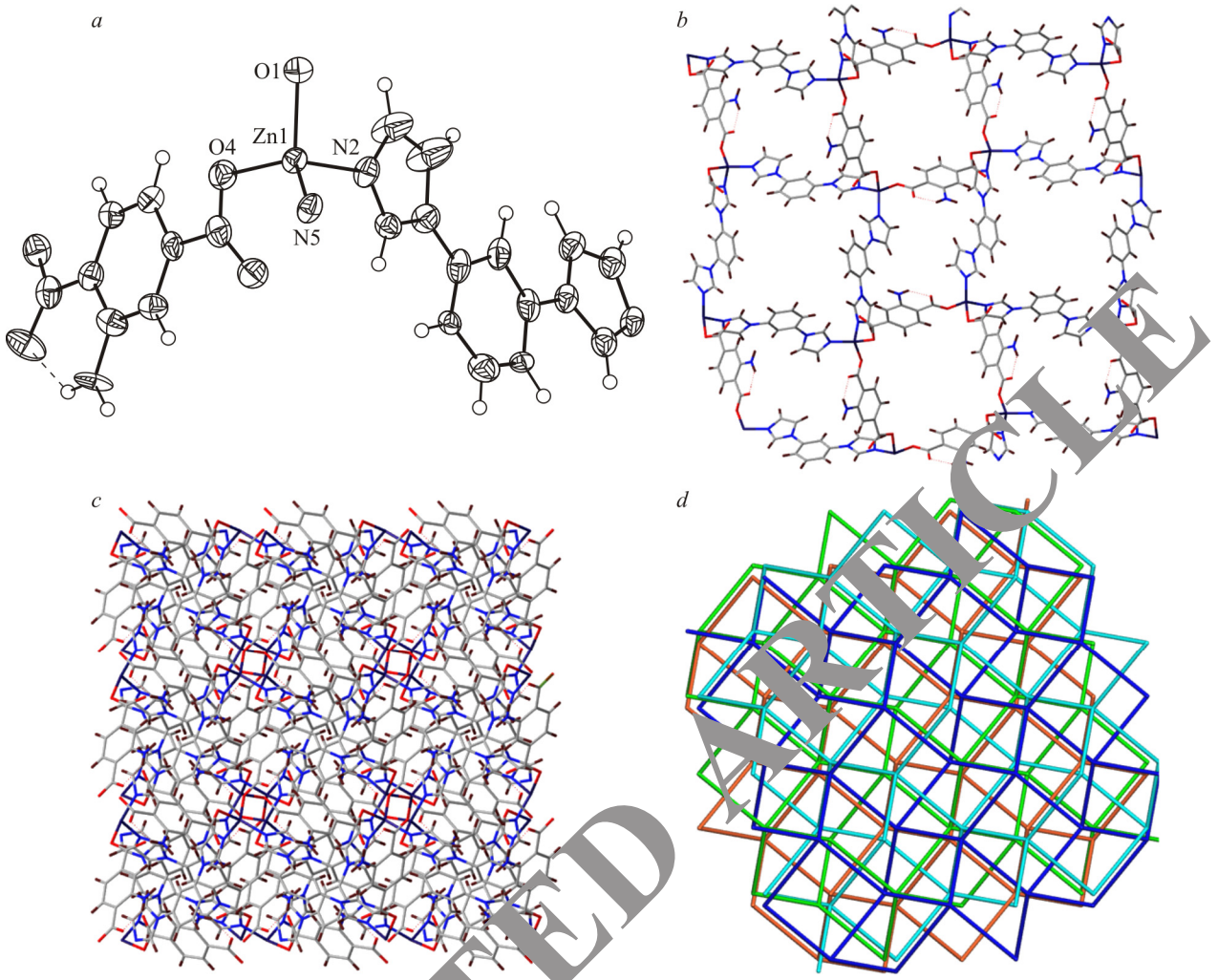

Fig. 2. Basic repeating unit for **2** (*a*); single network for **2** (*b*); 3D framework of **2** showing the nonporous structure (*c*); fourfold interpenetrated framework for **2** (*d*).

NH_2-bdc^{2-} ligands and two N atoms from two bib ligands, forming a distorted tetrahedral coordination surrounding. Notably, each four-coordinated Zn(II) ion is connected by two NH_2-bdc^{2-} ligands and two bib ligands to form a 3D neutral framework with a large porosity, which are large enough to include another three similar networks to form a closely packed network (Fig. 2*b*, *c*). Comparing with the coordination geometry of the Zn(II) cation in **1**, the Zn(II) cation in **2** is also in the tetrahedral environment. Thus, the overall topology of the framework of complex **2** can be simplified as a 4-connected 3D dia

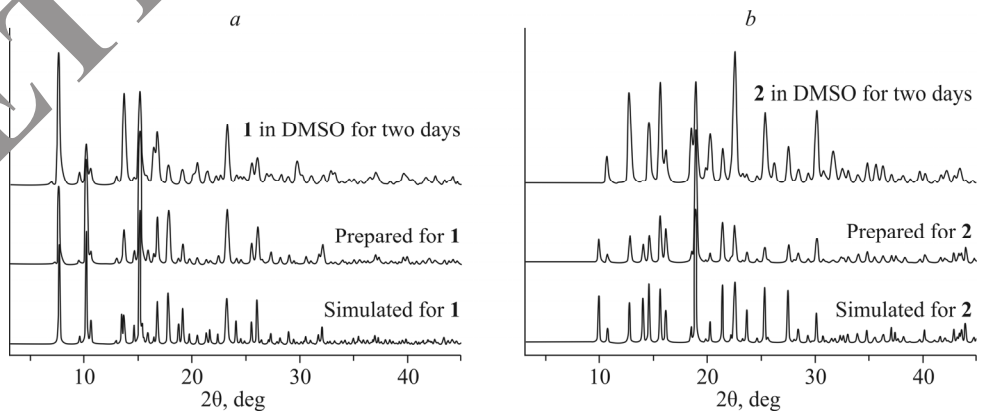

Fig. 3. PXRD patterns of **1** (*a*) and **2** (*b*).

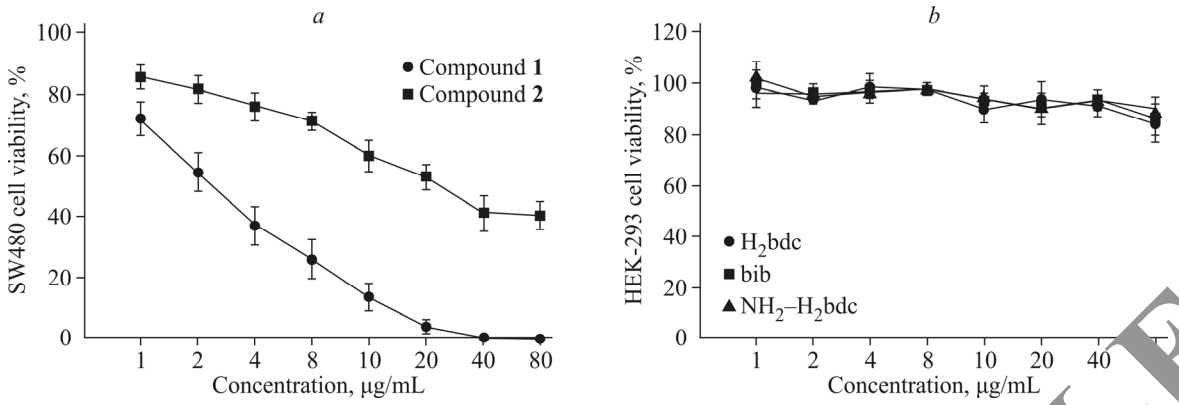

Fig. 4. Effect of compound **1** on the SW480 cell viability. The SW480 cells were exposed to different concentrations of compounds **1** and **2**; the cancer cell viability was measured by the CCK-8 assay (*a*). The cytotoxicity of H_2bdc, bib, and NH_2–H_2bdc ligands was assessed with the CCK-8 assay (*b*).

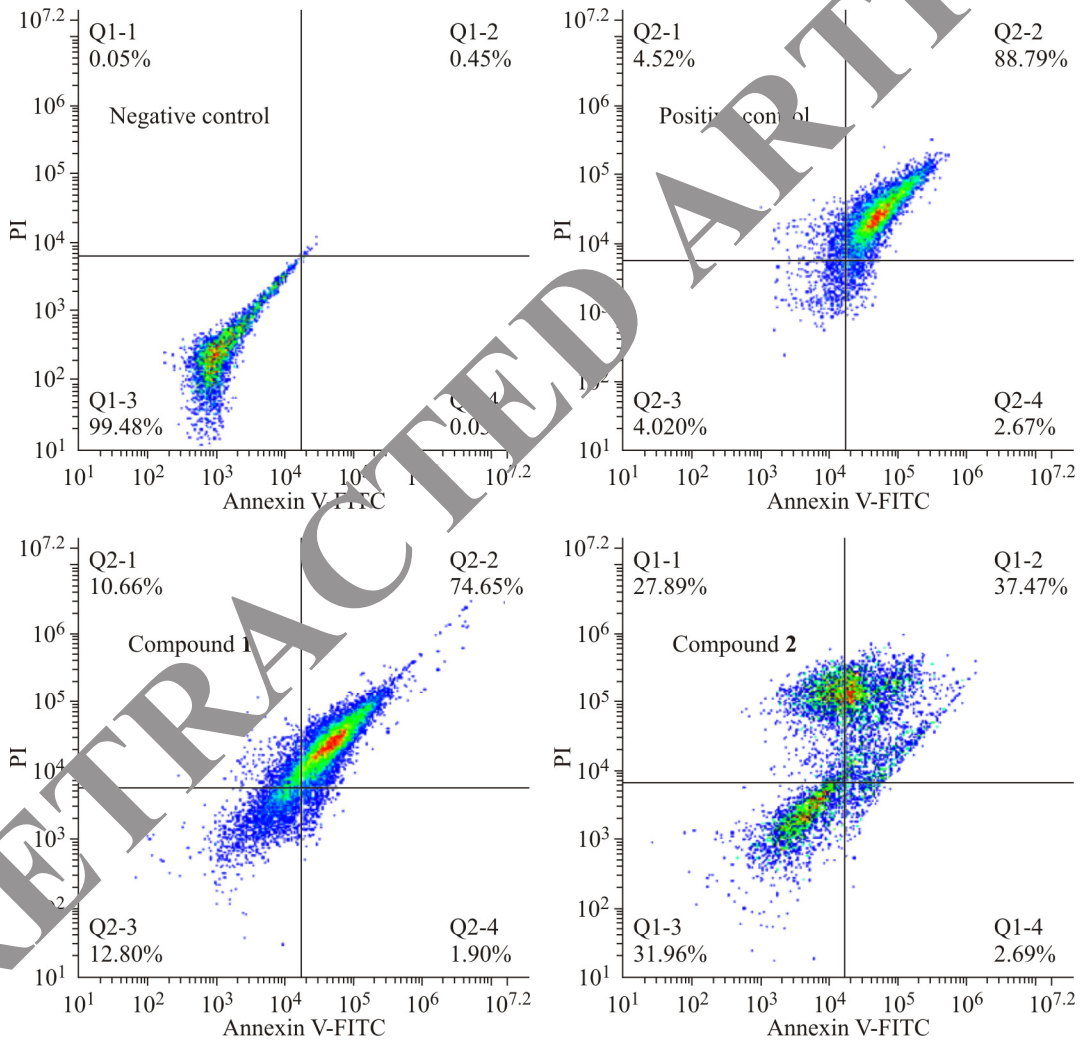

Fig. 5. Induction of apoptosis by compounds **1** and **2** in SW480 colon cancer cells. SW480 cells were treated with compounds **1** and **2**, then stained with Annexin V-FITC/PI, and analyzed by flow cytometry. The experiment was repeated at least three times.

network. Further, five such networks interpenetrate mutually to give a dense structure, making a fourfold interpenetrated framework (Fig. 2*d*). The π···π stacking interactions in complex **2** occur between bib and NH_2-bdc^{2-} ligands.

To confirm that the crystal structures are truly representative of the bulk materials, PXRD experiments were carried out for **1** and **2**. The experimental and simulated PXRD patterns of the corresponding compounds (Fig. 3) show that the bulk synthesized materials and the measured single crystals are the same. In view of the following bioactivity tests, it is necessary to study the stability of these two compounds in the DMSO solution. The freshly as-prepared two complexes were firstly ground in a mortar with a pestle for 1 h and then soaked in the DMSO solution for two days. Then the corresponding PXRD patterns were measured, which reflected that the PXRD patterns of the treated samples were comparable with those of the as-prepared samples, indicating their good framework stability in the DMSO solution.

Effect of the compounds on the SW480cell viability. The cytotoxic effects of compounds **1** and **2** on SW480 colon cancer cells were examined by the CCK-8 assay. The cells were exposed to various concentrations of the compounds for 24 and measured in a microplate reader. As the results show (Fig. 4), treatment with compound **1** significantly reduced the cancer cell viability in a dose-dependent manner. However, compound **2** could hardly reduce the SW480 cell viability (*a*). The H_2bdc, bib, and NH_2–H_2bdc ligands showed no cytotoxic activity on HEK-293 human cells (*b*).

Compound 1 induces apoptosis in SW480 colon cancer cells. To determine whether the apoptosis is responsible for the inhibition of the cell viability induced by compound **1**, the flow cytometry assay was performed. To quantify the SW480 colon cancer cell apoptosis, SW480 cells treated with compounds **1** and **2** were analyzed by flow cytometry. As shown in Fig. 5, the percentage of apoptotic cells increased to 74.65%, which was significantly higher than that after treatment with compound **2**. This indicated that compound **1** had a stronger ability in inducing SW480 cell apoptosis than compound **2**.

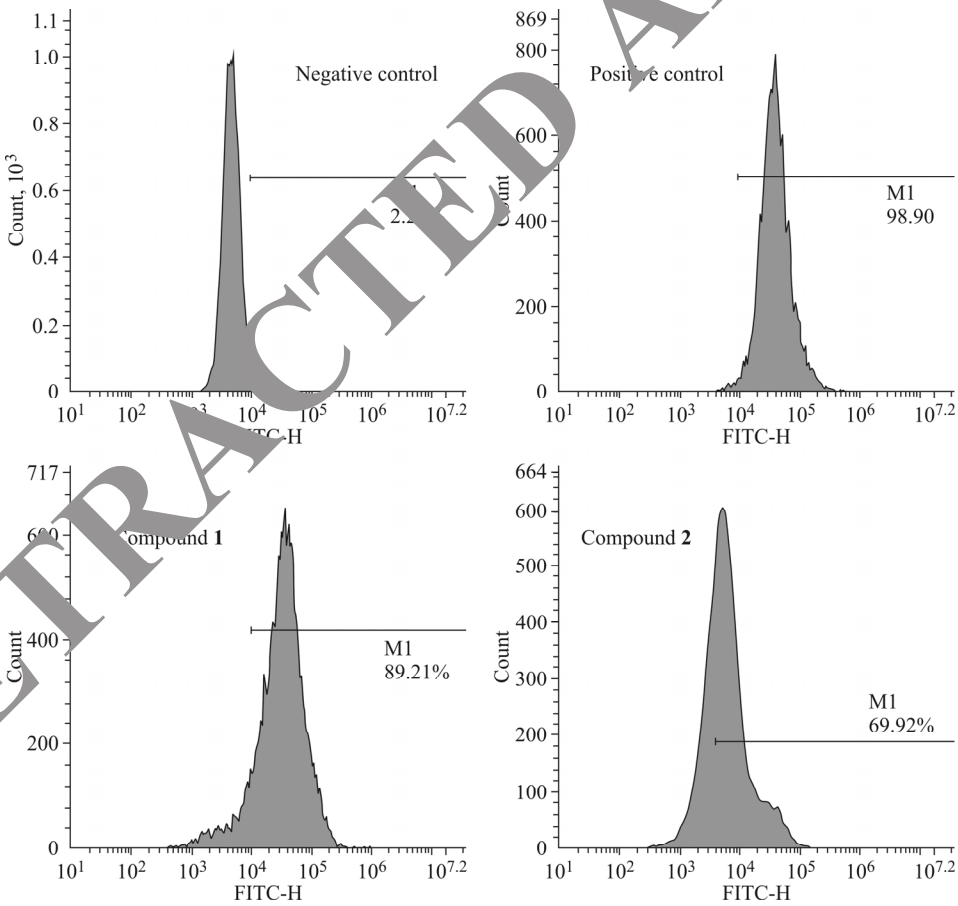

Fig. 6. Compound **1** induces the ROS production in SW480 colon cancer cells. After treating with compounds **1** and **2** at the same concentration, the intracellular ROS level was measured by the DCFH-DA assay. This experiment was performed in triplicate.

Compound 1 increases the intracellular ROS accumulation in SW480 colon cancer cells. The increased production of ROS was involved in the induction of cell apoptosis. Thus, we examined the ROS level in SW480 cells after treatment with compounds **1** and **2** by DCF fluorescence in flow cytometry. As shown in Fig. 6, compound **1** increased the level of SW480 intracellular ROS to 89.21%, which is notably higher than that after treatment with compound **2**.

CONCLUSIONS

In summary, we have obtained two mixed-ligand CPs by the reaction of zinc nitrate, N-containing and dicarboxylate ligands under the same hydrothermal conditions. Their structures have been fully studied via single crystal X-ray diffraction along with the elemental analysis. The structure solution and refinement results show that complex **1** has a 3D layered network with a 4-connected **sql** network, and complex **2** demonstrates a 3D diamond frameworks with a fourfold interpenetration. In addition, we explored the anticancer activity of compounds **1** and **2** in vitro, as well as its underlying mechanism. CKK-8 indicated the excellent anti-viability capability against SW480 colon cancer cells. The study of the mechanism reveals the anticancer activity of compound **1** due to the induction of ROS-mediated cell apoptosis, which provides a potential candidate for liver cancer treatment.

CONFLICT OF INTERESTS

The authors declare that they have no conflict of interests.

REFERENCES

1. Z. Mohseni Moghadam, R. Halabian, H. Sedighian, E. Behzadi, J. Am[illegible] and A. A. Imani Fooladi. *Iran J. Pathol*., **2019**, *14*, 305.
2. M. K. Kranjc, M. Novak, R. G. Pestell, and T. T. Lah. *Radiol. Oncol*., **2019**, *53*, 397.
3. C. W. Duan, L. X. Hu, and J. L. Ma. *J. Mater. Chem. A*, **2018**, *6*, 5309.
4. C. Duan, Y. Cao, L. Hu, D. Fu, J. Ma, and J. Youngblood. *J. Hazard. Mater*., **2019**, *373*, 141.
5. H. Wu, F. Chi, S. Zhang, J. Wen, J. Xiong, and S. [illegible] *Microporous Mesopor. Mat*., **2019**, *288*, 109567
6. X. Feng, N. Guo, H. P. Chen, H. L. Wang, [illegible] Y. Yue, X. Chen, S. W. Ng, X. F. Liu, L. F. Ma, and L. Y. Wang. *Dalton Trans*., **2017**, *46*, 14192.
7. X. Feng, J. G. Wang, B. Liu, L. Y. Wang, J. S. Zhao, and S. W. Ng. *Cryst. Growth Des*., **2012**, *12*, 927.
8. X. Feng, J. S. Zhao, B. Liu, L. Y. Wang, J. G. Wang, S. W. Ng, G. Zhang, X. G. Shi, and Y. Y. Liu. *Cryst. Growth Des*., **2010**, *10*, 1399.
9. Y. Q. Feng, Q. Zhao, and D. Q. [illegible] *Chin. J. Struct. Chem*., **2019**, *38*, 1909.
10. Y. Q. Feng, L. T. Jiang, and Z. Z. Xing, L. Wang. *Chin. J. Struct. Chem*., **2018**, *37*, 825.
11. J. Cheng, G. H. Wa[illegible] W. Wang. *J. Struct. Chem*., **2018**, *59*, 222.
12. S. W. Sun and G. F. Wang. *J. Struct. Chem*., **2019**, *60*, 466.
13. X. Yang, G. F. [illegible]ng, and L. Yang. *J. Struct. Chem*., **2018**, *59*, 1684.
14. J. P. Mo, L. Hasheni, J. L. He, W. L. Feng, Y. Yin, W. B. Zhang, X. H. Li, H. P. Xiao, and A. Morsali. *J. Mol. Struct*., **2019**, *1[illegible]*, 63[illegible]
15. Y. [illegible] Feng, S.Y. Chen, L. Wang, Z.Z. Xing. *Chin. J. Struct. Chem*., **2018**, *37*, 1656.
16. [illegible] Feng, M. Li, H. Fan, Q. Huang, D. Qiu, and H. Shi. *Dalton Trans*., **2015**, *44*, 894.
17. C. [illegible]antar, B. Kaya, M. Türk, and S. Şaşmaz. *J. Struct. Chem*., **2018**, 59, 1241.
18. X. N. Gao, E. J. Gao, and M. C. Zhu. *J. Struct. Chem*., **2019**, *60*, 1180.
19. L. J. Bourhis, O. V. Dolomanov, R. J. Gildea, J. A. K. Howard, and H. Puschmann. *Acta Crystallogr. A*, **2015**, *71*, 59.
20. O. V. Dolomanov, L. J. Bourhis, R. J. Gildea, J. A. K. Howard, and H. Puschmann. *J. Appl. Crystallogr*., **2009**, *42*, 339.
21. G. M. Sheldrick. *Acta Crystallogr. C*, **2015**, *71*, 3.